Upper and lower bound limit analysis of plates using FEM and second-order cone programming

Canh V. Le[*,a], H. Nguyen-Xuan[b], H. Nguyen-Dang[c]

[a] *Department of Civil and Structural Engineering, University of Sheffield, Sheffield S1 3JD, United Kingdom*
[b] *Department of Mechanics, Faculty of Mathematics and Computer Science, University of Science, VNU-HCM, 227 Nguyen Van Cu, Vietnam*
[c] *LTAS, Division of Fracture Mechanics, University of Liège, Bâtiment B52/3 Chemin des Chevreuils 1, B-4000 Liège 1, Belgium*

Abstract

This paper presents two novel numerical procedures to determine upper and lower bounds on the actual collapse load multiplier for plates in bending. The conforming Hsieh-Clough-Tocher (HCT) and enhanced Morley (EM) elements are used to discrete the problem fields. A Morley element with enhanced moment fields is used. The constant moment fields is added a quadratic mode in which the pressure is equilibrated by corner loads only, ensuring that exact equilibrium relations associated with a uniform pressure can be obtained. Once the displacement or moment fields are approximated and the bound theorems applied, limit analysis becomes a problem of optimization. In this paper, the optimization problems are formulated in the form of a standard second-order cone programming which can be solved using highly efficient interior point solvers. The procedures are tested by applying it to several benchmark plate problems and are found good agreement between the present upper and lower bound solutions and results in the literature.

Key words: Limit analysis, upper and lower bounds, displacement and equilibrium models, criterion of mean, second order cone programming

[*]Corresponding author
Email addresses: Canh.Le@sheffield.ac.uk (Canh V. Le), nxhung@hcmuns.edu.vn (H. Nguyen-Xuan), H.NguyenDang@ulg.ac.be (H. Nguyen-Dang)

1. Introduction

The yield line theory has been proved to be an effective method to perform plastic analysis of slabs and plates [1, 2]. This well-known method can predict very good upper-bound of the actual collapse multiplier for many practical engineering problems. However, this hand-based analysis method encounters difficulties in problems of arbitrary geometry, especially in the problems involving columns or holes. Consequently, over last few decades various numerical approaches based on bound theorems and mathematical programming have been developed [3, 4, 5, 6, 7, 8, 9, 10]. Numerical limit analysis generally involves two steps: (i) numerical discretization; and (ii) mathematical programming to enable a solution to be obtained. The finite element method, which is one of the most popular numerical methods, is often employed to discrete velocity or stress fields. Of several displacement and equilibrium elements that have been developed for Krichhoff plates in bending, the conforming Hsieh-Clough-Tocher (HCT) [11] and equilibrium Morley elements [12] are commonly utilized in practical engineering. The original HCT element will be used in the paper without any modification while the Morley element will be modified by adding a complementary field. Once the stress or displacement fields are approximated and the bound theorems applied, limit analysis becomes a problem of optimization involving either linear or nonlinear programming. Problems involving piecewise linear yield functions or nonlinear yield functions can respectively be solved using linear or non-linear programming techniques [13, 14, 5, 15, 16]. However, difficulty exists in the upper-bound optimization problem is that the objective function is convex, but not everywhere differentiable. One of the most efficient algorithms to overcome this singularity is the primal-dual interior-point method presented in [17, 18] and implemented in commercial codes such as the Mosek software package [19], such as second-order cone programming. The algorithm is also suitable for solving lower-bound limit analysis since most of yield conditions can be cast as a conic constraint [20]. These limit analysis problems can then be solved by this efficient algorithm [21, 22, 23].

In this paper two numerical procedures for upper and lower bound limit analysis of rigid-perfectly plastic plates governed by the von Mises criterion is proposed. A second degree moment field proposed by Debongnie and Nguyen-Xuan [24, 25, 26] is added to Morley moment fields to achieve exact equilibrium relations when applying a uniform pressure to plates. The enhanced Morley (EM) element will be adopted in the lower-bound limit analysis of plate problems. Attention is also focused on treating the performance of yield condition in numerical limit analysis. The criterion of mean proposed in [27] will be used instead of the exact criterion which is required to strictly satisfy. Due to this weakness of the yield condition we expect to obtain only an approximation of lower-bound in the statically admissible limit analysis. Attempts are also made by formulating both upper and lower bound limit analysis problems in terms of a standard second-order cone programming (SOCP). To illustrate the method it is then applied to a series of plate bending problems, including those for which solutions already exist in the literature.

2. Limit analysis formulations

2.1. Limit analysis duality theorems

Consider a rigid-perfectly plastic body of volume $\Omega \in \mathbb{R}^3$ with boundary Γ. Let Γ_u and Γ_g denote, respectively, an essential boundary (Dirichlet condition) where displacement boundary conditions are prescribed and a natural boundary (Neumann condition) where stress boundary conditions are assumed, $\Gamma_u \cup \Gamma_g = \Gamma$. The external loads which are denoted by g and f, respectively subject to surface and volume of the body. Let $\dot{\mathbf{u}}$ be a plastic velocity or flow field that belongs to a space Y of kinematically admissible velocity fields and $\boldsymbol{\sigma}$ be a stress field belonging to an appropriate space of symmetric stress tensor X. The mathematical formulations for limit analysis will be briefly described in this section. More details can be found in [28, 22, 23].

The external work rate of forces (g, f) associated with a virtual plastic flow

$\dot{\mathbf{u}}$ is expressed in the linear form as

$$F(\dot{\mathbf{u}}) = \int_{\Omega} f\dot{\mathbf{u}}\,\mathrm{d}\Omega + \int_{\Gamma_g} g\dot{\mathbf{u}}\,\mathrm{d}\Gamma \tag{1}$$

The internal work rate for sufficiently smooth stresses $\boldsymbol{\sigma}$ and velocity fields $\dot{\mathbf{u}}$ is given by the bilinear form

$$a(\boldsymbol{\sigma}, \dot{\mathbf{u}}) = \int_{\Omega} \boldsymbol{\sigma}^T \dot{\boldsymbol{\epsilon}}(\dot{\mathbf{u}})\,\mathrm{d}\Omega \tag{2}$$

where $\dot{\boldsymbol{\epsilon}}(\dot{\mathbf{u}})$ are strain rates.

The equilibrium equation is then described in the form of virtual work rate as follows

$$a(\boldsymbol{\sigma}, \dot{\mathbf{u}}) = F(\dot{\mathbf{u}}), \forall \dot{\mathbf{u}} \in Y \text{ and } \dot{\mathbf{u}} = 0 \text{ on } \Gamma_u \tag{3}$$

Furthermore, the stresses $\boldsymbol{\sigma}$ must satisfy the yield condition for assumed material. This stress field belongs to a convex set, B, obtaining from the used field condition. For the von Mises criterion,

$$B = \{\boldsymbol{\sigma} \in X \mid s_{ij}s_{ij} \leq 2k^2\} \tag{4}$$

where s_{ij} denotes stress deviator tensor and k is a parameter depending on material properties.

If defining $C = \{\dot{\mathbf{u}} \in Y \mid F(\dot{\mathbf{u}}) = 1\}$, the exact collapse multiplier λ_{exact} can be determined by solving any of the following optimization problems

$$\begin{aligned}
\lambda_{exact} &= \max\{\lambda \mid \exists\, \boldsymbol{\sigma} \in B :\ a(\boldsymbol{\sigma}, \dot{\mathbf{u}}) = \lambda F(\dot{\mathbf{u}}), \forall \dot{\mathbf{u}} \in Y\} && (5)\\
&= \max_{\boldsymbol{\sigma} \in B} \min_{\dot{\mathbf{u}} \in C} a(\boldsymbol{\sigma}, \dot{\mathbf{u}}) && (6)\\
&= \min_{\dot{\mathbf{u}} \in C} \max_{\boldsymbol{\sigma} \in B} a(\boldsymbol{\sigma}, \dot{\mathbf{u}}) && (7)\\
&= \min_{\dot{\mathbf{u}} \in C} D(\dot{\mathbf{u}}), && (8)
\end{aligned}$$

where $D(\dot{\mathbf{u}}) = \max_{\boldsymbol{\sigma} \in B} a(\boldsymbol{\sigma}, \dot{\mathbf{u}})$ is the plastic dissipation rate. Problems (5) and (8) are knows as static and kinematic principles of limit analysis, respectively. The

limit load of both approaches converges to the exact solution. Herein, a saddle point $(\boldsymbol{\sigma}^*, \dot{\mathbf{u}}^*)$ exists such that both the maximum of all lower bounds λ^- and the minimum of all upper bounds λ^+ coincide and are equal to the exact value λ_{exact}.

2.2. Formulations for plates

Considers a plate bounded by a curve enclosing a plane area A with kinematical boundary $\Gamma_w \cup \Gamma_{w_n}$ and static boundary $\Gamma_m \cup \Gamma_{m_n}$, where the subscript n stands for outward normal. The general relations for limit analysis of thin plates associated with Kirchhoff's hypothesis are given as follows.

Equilibrium: Collecting the bending moments in the vector $\mathbf{m}^T = [m_{xx} \;\; m_{yy} \;\; m_{xy}]$, the equilibrium equations can be written as

$$(\nabla^2)^T \mathbf{m} + \lambda p = 0 \tag{9}$$

where p is the transverse load and the differential operator ∇^2 is defined by $\nabla^2 = [\dfrac{\partial^2}{\partial x^2} \;\; \dfrac{\partial^2}{\partial y^2} \;\; 2\dfrac{\partial^2}{\partial x \partial y}]^T$.

Compatibility: If w denotes the transverse displacement, the curvature rates can be expressed by relations

$$\dot{\boldsymbol{\kappa}} = -[\dot{\kappa}_{xx} \;\; \dot{\kappa}_{yy} \;\; 2\dot{\kappa}_{xy}]^T = -\nabla^2 \dot{w} \tag{10}$$

Flow rule and yield condition: In framework of a limit analysis problem, only plastic strains (curvatures) are considered and are assumed to obey the normality rule $\dot{\boldsymbol{\kappa}} = \dot{\mu} \dfrac{\partial \psi}{\partial \mathbf{m}}$, where the plastic multiplier $\dot{\mu}$ is non-negative and the yield function $\psi(\mathbf{m})$ is convex. In this study, the von Mises failure criterion in the space of moment components is used

$$\psi(\mathbf{m}) = \sqrt{\mathbf{m}^T \; \mathbf{P} \; \mathbf{m}} - m_p \leq 0 \tag{11}$$

where $m_p = \sigma_0 t^2/4$ is the plastic moment of resistance per unit width of a plate of uniform thickness t, σ_0 is the yield stress and

$$\mathbf{P} = \frac{1}{2}\begin{bmatrix} 2 & -1 & 0 \\ -1 & 2 & 0 \\ 0 & 0 & 6 \end{bmatrix} \tag{12}$$

The dissipation rate: The internal dissipation power of the two-dimensional plate domain A can be written as a function of curvature rates as

$$D(\dot{\boldsymbol{\kappa}}) = \int_A \int_{-t/2}^{t/2} \sigma_0 \sqrt{\dot{\boldsymbol{\epsilon}}^T \mathbf{Q} \dot{\boldsymbol{\epsilon}}}\, \mathrm{d}z\, \mathrm{d}A = m_p \int_A \sqrt{\dot{\boldsymbol{\kappa}}^T \mathbf{Q}\, \dot{\boldsymbol{\kappa}}}\, \mathrm{d}A \tag{13}$$

where

$$\dot{\boldsymbol{\epsilon}} = \begin{bmatrix} \dot{\epsilon}_{xx} \\ \dot{\epsilon}_{yy} \\ \dot{\gamma}_{xy} \end{bmatrix} = z\dot{\boldsymbol{\kappa}} \tag{14}$$

$$\mathbf{Q} = \mathbf{P}^{-1} = \frac{1}{3}\begin{bmatrix} 4 & 2 & 0 \\ 2 & 4 & 0 \\ 0 & 0 & 1 \end{bmatrix} \tag{15}$$

Details on the derivation of the dissipation for plate problems can be found in [6, 29].

3. Finite element discretezation

3.1. Lower-bound formulation

In numerical lower-bound limit analysis problem, a statically admissible stress or moment field for an individual element is chosen so that equilibrium equations and stress continuity requirements within the element and along its boundaries are met. The well-known equilibrium Morley element with constant varying moment is the simplest model for practical engineering. It is, therefore, advantage to extent the use of the element to lower-bound limit analysis problem in this paper. The moment field $\mathbf{m}$ is assumed to vary constantly within

an element and expressed as

$$\mathbf{m} = \mathbf{I}\boldsymbol{\beta} \tag{16}$$

where $\mathbf{I}$ is a identity matrix and $\boldsymbol{\beta} = [\beta_1 \ \beta_2 \ \beta_3]^T$ is an unknown vector.

The generalized loads comprise three corner loads Z_1, Z_2, Z_3 and three normal moments bending along edges m_{12}, m_{23}, m_{31} as shown in Figure 1. All generalized loads can be expressed in terms of moment parameters, if $\mathbf{G}$ denotes the generalized vector, the relations are written as

$$\mathbf{G} = \mathbf{C}\boldsymbol{\beta} \tag{17}$$

where

$$\mathbf{G} = \begin{bmatrix} Z_1 & Z_2 & Z_3 & m_{12} & m_{23} & m_{31} \end{bmatrix}^T \tag{18}$$

$$\mathbf{C} = \begin{bmatrix} c_3 s_3 - c_1 s_1 & c_1 s_1 - c_3 s_3 & c_1^2 - s_1^2 - c_3^2 + s_3^2 \\ c_1 s_1 - c_2 s_2 & c_2 s_2 - c_1 s_1 & c_2^2 - s_2^2 - c_1^2 + s_1^2 \\ c_2 s_2 - c_3 s_3 & c_3 s_3 - c_2 s_2 & c_3^2 - s_3^2 - c_2^2 + s_2^2 \\ c_1^2 L_{12} & s_1^2 L_{12} & c_1 s_1 L_{12} \\ c_2^2 L_{23} & s_2^2 L_{23} & c_2 s_2 L_{23} \\ c_3^2 L_{32} & s_3^2 L_{32} & c_3 s_3 L_{32} \end{bmatrix} \tag{19}$$

in which the direction cosines of the outward normal to the element boundary $(c_i,\ s_i)$ are determined as

$$c_i = \frac{y_j - y_i}{L_{ij}}, \quad s_i = \frac{x_i - x_j}{L_{ij}}, \quad ij = 12,\ 23,\ 31 \tag{20}$$

and L_{ij} is the length of edge ij.

It is important to note that, in the case when a uniform pressure is applied, the Morley element does not result in a exact equilibrium relation. This is because the equation (9) does not hold with the use of the constant moment fields. It is, therefore, necessary to add to the constant moment fields by a particular higher degree solution which has to be such chosen that side loads

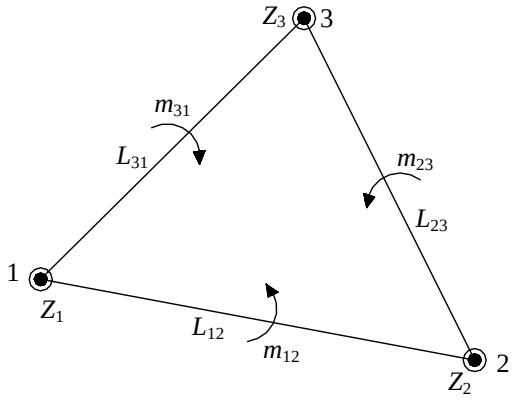

Figure 1: Morley equilibrium element

are compatible with the original element. A second degree moment field which can be added to equilibrium elements of either degree one or degree zero has been proposed by [24, 25, 26] and can be expressed as

$$\mathbf{m}_c = \lambda p \, a_e \, \mathbf{T} \tag{21}$$

where a_e is the area of an element and $\mathbf{T} = [T_{xx} \; T_{yy} \; T_{xy}]^T$ and is given as

$$\mathbf{T} = -\frac{1}{3} \begin{bmatrix} -\dfrac{\mathrm{X}_3}{\mathrm{Y}_3}k_1 + \dfrac{\mathrm{X}_3 - \mathrm{X}_2}{\mathrm{Y}_3}k_2 - \dfrac{\mathrm{X}_3(\mathrm{X}_3 - \mathrm{X}_2)}{\mathrm{Y}_3\mathrm{X}_2}k_3 + \dfrac{1}{2a_e}(\mathrm{X}^2 - \mathrm{X}_2^2 k_2 - \mathrm{X}_3^2 k_3) \\ -\dfrac{\mathrm{Y}_3}{\mathrm{X}_2}k_3 + \dfrac{1}{2a_e}(\mathrm{Y}^2 - \mathrm{Y}_3^2 k_3) \\ -\dfrac{1}{2}k_1 + \dfrac{1}{2}k_2 - \dfrac{2\mathrm{X}_3 - \mathrm{X}_2}{2\mathrm{X}_2}k_3 + \dfrac{1}{2a_e}(\mathrm{XY} - \mathrm{X}_3\mathrm{Y}_3 k_3) \end{bmatrix} \tag{22}$$

This complementary mode is constructed based on a particular system of axes as shown in Figure 2, in which the side 1-2 is chosen to be the X axis and Y must go through node 1 and is orientated so that Y_3 is positive. Three area coordinates are denoted by k_1(X,Y), k_2(X,Y) and k_3(X,Y). The modified Morley element was called as enhanced Morley (EM) element by [26].

Similarly, the three generalized loads at corners of the triangular element

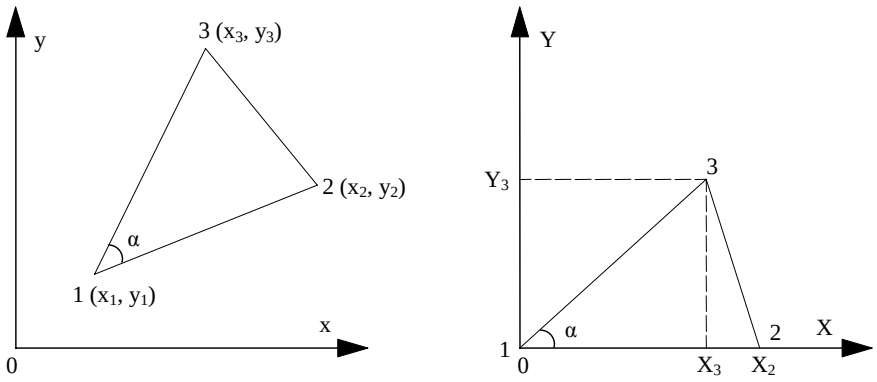

Figure 2: Relations between global system (Oxy) and local system (OXY)

are added by $-\frac{a_e p}{3}$. The equilibrium equation Eq. (17) is then rewritten as

$$\mathbf{G} = \overline{\mathbf{C}}\ \overline{\boldsymbol{\beta}} \tag{23}$$

where

$$\begin{aligned}
\overline{\boldsymbol{\beta}} &= \begin{bmatrix} \beta_1 & \beta_2 & \beta_3 & \lambda \end{bmatrix} \\
\overline{\mathbf{C}} &= \begin{bmatrix}
c_3 s_3 - c_1 s_1 & c_1 s_1 - c_3 s_3 & c_1^2 - s_1^2 - c_3^2 + s_3^2 & -\dfrac{p\, a_e}{3} \\
c_1 s_1 - c_2 s_2 & c_2 s_2 - c_1 s_1 & c_2^2 - s_2^2 - c_1^2 + s_1^2 & -\dfrac{p\, a_e}{3} \\
c_2 s_2 - c_3 s_3 & c_3 s_3 - c_2 s_2 & c_3^2 - s_3^2 - c_2^2 + s_2^2 & -\dfrac{p\, a_e}{3} \\
c_1^2 L_{12} & s_1^2 L_{12} & c_1 s_1 L_{12} & 0 \\
c_2^2 L_{23} & s_2^2 L_{23} & c_2 s_2 L_{23} & 0 \\
c_3^2 L_{32} & s_3^2 L_{32} & c_3 s_3 L_{32} & 0
\end{bmatrix}
\end{aligned} \tag{24}$$

The overall equilibrium for the structure can be obtained by assembling all local equilibrium equations of elements and expressed as

$$\mathbf{C}_s\ \boldsymbol{\beta}_s = 0 \tag{25}$$

with $\boldsymbol{\beta}_s = [\beta_1\ \ \beta_2\ \ \ldots \beta_{3*nele}\ \ \lambda]$, *nele* is the number of elements. Notes that

boundary conditions are also imposed here in the assemble scheme.

Furthermore, the modified moment field $\overline{\mathbf{m}}$ is not allowed to violate the yield condition

$$\psi(\overline{\mathbf{m}}) = \sqrt{\overline{\mathbf{m}}^T \, \mathbf{P} \, \overline{\mathbf{m}}} - m_p \leq 0 \tag{26}$$

where

$$\overline{\mathbf{m}} = \boldsymbol{\beta} + \lambda p \, a_e \mathbf{T} \tag{27}$$

However, in numerical analysis it is not always possible to satisfy this requirement since the yield condition is commonly fulfilled at Gauss points or nodes. Instead of strictly satisfying the exact criterion, Nguyen-Dang proposed the criterion of mean [27, 30] which is satisfied locally within element domains. For plate problem the criterion of mean can be expressed as

$$\frac{1}{a_e} \int_{a_e} \sqrt{\overline{\mathbf{m}}^T \, \mathbf{P} \, \overline{\mathbf{m}}} \, \mathrm{d}a - m_p \leq 0 \tag{28}$$

Introducing the smoothed value of $\overline{\mathbf{m}}$ the Eq. (28) can be rewritten as

$$\psi(\boldsymbol{\rho}) = \sqrt{\boldsymbol{\rho}^T \, \mathbf{P} \, \boldsymbol{\rho}} - m_p \leq 0 \tag{29}$$

where $\boldsymbol{\rho}$ is the smoothed version of $\overline{\mathbf{m}}$ and given by

$$\boldsymbol{\rho} = \frac{1}{a_e} \int_{a_e} \overline{\mathbf{m}} \, \mathrm{d}a = \boldsymbol{\beta} + \lambda p \int_{a_e} \mathbf{T} \, \mathrm{d}a = \boldsymbol{\beta} + \lambda p \, \mathbf{S} \tag{30}$$

in which $\mathbf{S}$ is the exact integration of $\int_{a_e} \mathbf{T} \, \mathrm{d}a$ in the local coordinate OXY.

If defining $B_i = \{\boldsymbol{\rho}_i \mid \psi(\boldsymbol{\rho}_i) \leq 0\}$ is the set of admissible discrete moments for each element, the lower-bound limit analysis (5) can be now written in terms of discrete moment space as

$$\begin{aligned} \lambda^- \quad = \quad & \max \ \lambda \\ & \text{s.t} \begin{cases} \mathbf{C}_s \ \boldsymbol{\beta}_s = 0 \\ \boldsymbol{\rho}_i = \boldsymbol{\beta}_i + \lambda p \, \mathbf{S}_i \\ \boldsymbol{\rho}_i \in B_i, \ i = 1, \ 2, \ \ldots, \ nele \end{cases} \end{aligned} \tag{31}$$

and accompanied by appropriate boundary conditions.

3.2. Upper-bound formulation

In numerical upper-bound limit analysis of plate problem, the velocity field with an element is represented by a continuous function expressed in terms of spatial coordinates and nodal values. For Krichhoff plates, an element of class C^1 should be employed to approximate the velocity field. The conforming Hsieh-Clough-Tocher (HCT) triangular element will be utilized and briefly summarized in this section. A triangular element is subdivided into 3 sub-elements using individual cubic expansions over each sub-element as shown in Figure 3. The element has 12 degrees of freedom: the transverse displacements and 2 the rotation components at each corner node (w_i, $\theta_{xi} = \partial w_i/\partial x\,|_i$, $\theta_{yi} = \partial w_i/\partial y\,|_i$, $i =$ 1, 2, 3) and normal rotations at 3 mid-side nodes ($\theta_i = \partial w_i/\partial n\,|_i$, $i = 4, 5, 6$).

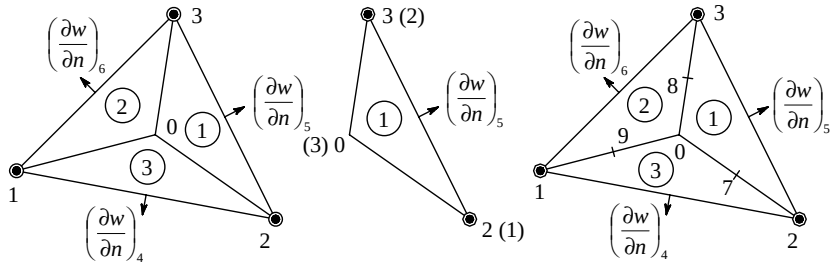

Figure 3: HCT element

The displacement expansion $w^{(k)}$ can be expressed in terms of area coordinates $\boldsymbol{\zeta} = (\zeta_1, \zeta_2, \zeta_3)$ over each sub-triangle as

$$w^{(k)}(\boldsymbol{\zeta}) = \left(\mathbf{N}_e^{(k)}(\boldsymbol{\zeta}) + \mathbf{N}_0^{(k)}(\boldsymbol{\zeta})\mathbf{F}\right)\,\mathbf{q}_e,\ k = 1, 2, 3 \tag{32}$$

where the partitions $\mathbf{N}_e^{(k)}(\boldsymbol{\zeta})$ and $\mathbf{N}_0^{(k)}(\boldsymbol{\zeta})$ respectively represent the interpolation functions associated with element displacements $\mathbf{q}_e$ and internal nodal displacements and $\mathbf{F}$ is the matrix of elimination obtained by applying compatible requirements at internal nodes 7, 8, 9.

The plastic dissipation for a sub-element is now formulated as

$$D^{(k)}(\boldsymbol{\kappa}^{(k)}) = m_p \int_{A_{se}} \sqrt{\dot{\boldsymbol{\kappa}}^T \mathbf{Q}\ \dot{\boldsymbol{\kappa}}}\, \mathrm{d}A = m_p \sum_{j=1}^{ng} \xi_j \sqrt{\dot{\boldsymbol{\kappa}}^T(\boldsymbol{\zeta}_j)\mathbf{Q}\ \dot{\boldsymbol{\kappa}}(\boldsymbol{\zeta}_j)} \tag{33}$$

where $ng = 3$ is the number of Gauss integration points in each sub-element $A^{(k)}$, ξ_j is the weighting factor of the Gauss point $\boldsymbol{\zeta}_j$ and $\boldsymbol{\kappa}^{(k)}(\boldsymbol{\zeta}_j)$ are curvatures at the Gauss point $\boldsymbol{\zeta}_j$

$$\dot{\boldsymbol{\kappa}}^{(k)}(\boldsymbol{\zeta}_j) = \begin{bmatrix} \dot{\kappa}^{(k)}_{xx}(\boldsymbol{\zeta}_j) \\ \dot{\kappa}^{(k)}_{yy}(\boldsymbol{\zeta}_j) \\ \dot{\kappa}^{(k)}_{xy}(\boldsymbol{\zeta}_j) \end{bmatrix} = \begin{bmatrix} \mathbf{N}^{(k)}_{e,xx}(\boldsymbol{\zeta}_j) + \mathbf{N}^{(k)}_{0,xx}(\boldsymbol{\zeta}_j)\mathbf{F} \\ \mathbf{N}^{(k)}_{e,yy}(\boldsymbol{\zeta}_j) + \mathbf{N}^{(k)}_{0,yy}(\boldsymbol{\zeta}_j)\mathbf{F} \\ \mathbf{N}^{(k)}_{e,xy}(\boldsymbol{\zeta}_j) + \mathbf{N}^{(k)}_{0,xy}(\boldsymbol{\zeta}_j)\mathbf{F} \end{bmatrix} \dot{\mathbf{q}}_e \tag{34}$$

By summing all dissipations of all sub-elements and elements, the plastic dissipation of the whole plate is

$$D = m_p \sum^{nele} \sum^{3} \sum_{j=1}^{ng} \xi_j \sqrt{\dot{\boldsymbol{\kappa}}^T(\boldsymbol{\zeta}_j)\mathbf{Q}\ \dot{\boldsymbol{\kappa}}(\boldsymbol{\zeta}_j)} \tag{35}$$

Similarly, the work rate of applied loads can be expressed as

$$F = \sum^{nele} \sum^{3} \sum_{j=1}^{ng} \xi_j p\, \dot{w}^{(k)}(\boldsymbol{\zeta}_j) \tag{36}$$

The upper-bound limit analysis of plate bending is now written as

$$\begin{aligned} \lambda^+ \quad = \quad & \min\ m_p \sum^{nele} \sum^{3} \sum_{j=1}^{ng} \xi_j \sqrt{\dot{\boldsymbol{\kappa}}^T(\boldsymbol{\zeta}_j)\mathbf{Q}\ \dot{\boldsymbol{\kappa}}(\boldsymbol{\zeta}_j)} \\ & \text{s.t} \begin{cases} \displaystyle\sum^{nele} \sum^{3} \sum_{j=1}^{ng} \xi_j p\, \dot{w}^{(k)}(\boldsymbol{\zeta}_j) = 1 \\ \dot{\mathbf{q}} = 0 \text{ on } \Gamma_w \end{cases} \end{aligned} \tag{37}$$

4. Second-order cone programming

4.1. Conic programming

The general form of a Second-Order Cone Programming (SOCP) problem with N sets of constraints is written as follows

$$\min \ \mathbf{f}^T\mathbf{x}$$

$$\text{s. t. } \|\mathbf{H}_i\mathbf{x}+\mathbf{v}_i\| \leq \mathbf{y}_i^T\mathbf{x}+z_i \text{ for } i=1,\ldots,N \tag{38}$$

where $\mathbf{x}\in\mathbb{R}^n$ are the optimization variables, and the problem coefficients are $\mathbf{f}\in\mathbb{R}^n$, $\mathbf{H}_i\in\mathbb{R}^{m\times n}$, $\mathbf{v}_i\in\mathbb{R}^m$, $\mathbf{y}_i\in\mathbb{R}^n$, and $z_i\in\mathbb{R}$. For optimization problems in 2D or 3D Euclidean space, $m=2$ or $m=3$. When $m=1$ the SOCP problem reduces to a linear programming problem. In framework of limit analysis problems, the two most common second-order cones are the quadratic cone

$$\mathscr{C}_q=\left\{\mathbf{x}\in\mathbb{R}^{k+1} \mid x_1\geq\sqrt{\sum_{j=2}^{k+1}x_j^2}=\|\mathbf{x}_{2\to k+1}\|\right\} \tag{39}$$

and the rotated quadratic cone

$$\mathscr{C}_r=\left\{\mathbf{x}\in\mathbb{R}^{k+2} \mid x_1x_2\geq\sum_{j=3}^{k+2}x_j^2=\|\mathbf{x}_{3\to k+2}\|^2,\ x_1,\,x_2\geq 0\right\} \tag{40}$$

4.2. Lower-bound programming

Since the matrix $\mathbf{P}$ is a positive definite matrix, the constraint (29) can be cast in terms of a conic quadratic constraint as

$$\boldsymbol{\rho}\in\mathscr{C}_q,\quad \mathscr{C}_q=\left\{\boldsymbol{\rho}\in\mathbb{R}^4 \mid \rho_4\geq\|\mathbf{J}_1^T\boldsymbol{\rho}_{1\to 3}\|,\ \rho_4=m_p\right\} \tag{41}$$

where $\mathbf{J}_1$ is the so-called Cholesky factor of $\mathbf{P}$

$$\mathbf{J}_1 = \frac{1}{2}\begin{bmatrix} 2 & 0 & 0 \\ -1 & \sqrt{3} & 0 \\ 0 & 0 & 2\sqrt{3} \end{bmatrix} \tag{42}$$

The lower-bound limit analysis of plates is then cast in the form of a second-order cone programming as

$$\begin{aligned} \lambda^- \quad = \quad & \max\ \lambda \\ & \text{s.t} \begin{cases} \mathbf{C}_s\ \boldsymbol{\beta}_s = 0 \\ \boldsymbol{\rho}_i = \boldsymbol{\beta}_i + \lambda p\, \mathbf{S}_i \\ \boldsymbol{\rho}_i \in \mathscr{C}_q^i,\ i = 1,\ 2,\ \ldots,\ nele \end{cases} \end{aligned} \tag{43}$$

and accompanied by appropriate boundary conditions.

4.3. Upper-bound programming

In order to cast the optimization problem (37) in the form of a standard second-order cone programming, its objective function is firstly formulated in a form involving a sum of norms as

$$m_p \sum^{nele}\sum^{3}\sum_{j=1}^{ng} \xi_j \sqrt{\dot{\boldsymbol{\kappa}}^T(\boldsymbol{\zeta}_j)\mathbf{Q}\ \dot{\boldsymbol{\kappa}}(\boldsymbol{\zeta}_j)} = m_p \sum^{nele}\sum^{3}\sum_{j=1}^{ng} \xi_j \|\mathbf{J}_2^T\ \dot{\boldsymbol{\kappa}}(\boldsymbol{\zeta}_j)\| \tag{44}$$

where $\mathbf{J}_2$ is the Cholesky factor of $\mathbf{Q}$

$$\mathbf{J}_2 = \frac{1}{\sqrt{3}}\begin{bmatrix} 2 & 0 & 0 \\ 1 & \sqrt{3} & 0 \\ 0 & 0 & 1 \end{bmatrix} \tag{45}$$

By introducing auxiliary variables $t_1,\ t_2,\ \ldots,\ t_{nele\times 3\times ng}$ the present upper-bound optimization problem can be rewritten in the form of a standard SOCP

problem as

$$\lambda^{+} \;=\; \min\; m_p \sum_{k}^{nele\times 3\times ng} \xi_k t_k$$
$$\text{s.t}\begin{cases} \sum^{nele}\sum^{3}\sum_{j=1}^{ng} \xi_j p\, \dot{w}^{(k)}(\boldsymbol{\zeta}_j) = 1 \\ \dot{\mathbf{q}} = 0 \text{ on } \Gamma_w \\ \mathbf{r}_i = \mathbf{J}_2^T\, \dot{\boldsymbol{\kappa}} \\ \|\mathbf{r}_i\| \leq t_i, \quad i = 1, 2, \ldots, nele \times 3 \times ng \end{cases} \tag{46}$$

in which $\|\mathbf{r}_i\| \leq t_i$ expresses quadratic cones and $\mathbf{r}_i$ are additional variables, where every $\mathbf{r}_i$ is a 3×1 vector. The total number of variables of this optimization problem is $sdof + 4 \times 3 \times ng \times nele$; $sdof$ is the degrees of freedom of system.

5. Numerical examples

The numerical performance of the procedures are illustrated by applying it to uniformly loaded plate problems for which, in most cases, solutions already exist in the literature (the method is applicable to problems of arbitrary geometry). For all the examples considered the following was assumed: length $L = 10$ m; plate thickness $t = 0.1$ m; yield stress $\sigma_0 = 250$ MPa. Quarter symmetry was assumed when appropriate. Note that, solutions obtained in the static problems are approximations of lower-bound due to criterion of the mean was used. However, as the discretization is sufficiently fine, increasingly close approximations of the true plastic collapse load multiplier can be expected to be obtained.

The first examples is a square plate with clamped supports and subjected to uniform out-of-plane pressure loading. This problem was solved by the top-right quarter of the plate and uniform mesh generation was used, see Figure 4. Matlab optimization toolbox 3.0 and Mosek version 5.0 optimization solvers were used to obtain solutions (using a 2.8 GHz Pentium 4 PC running Microsoft XP).

The efficacy of various optimization algorithms was firstly considered. The

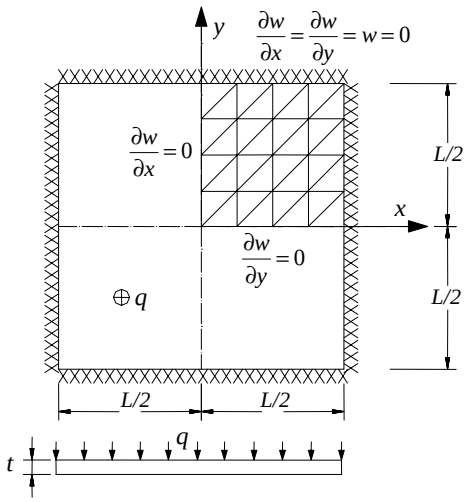

Figure 4: Square plate clamped along edges and loaded by a uniformly pressure

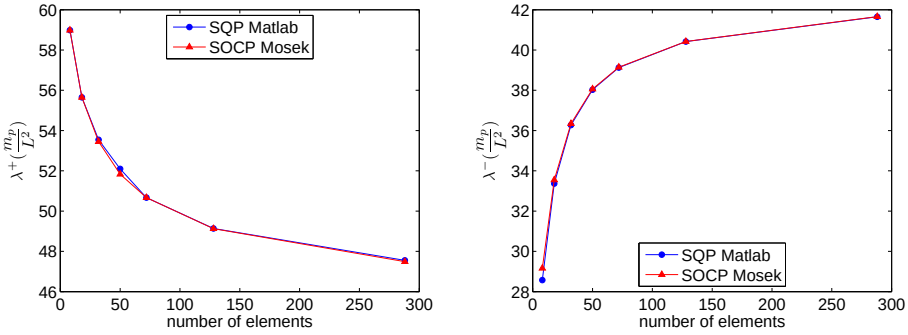

(a) Upper-bound (b) Lower-bound

Figure 5: Comparison the performance of SQP and SOCP

limit analysis problems (31) and (37) are typically non-linear optimization problems and it can be solved using a general non-linear optimization solver, such as a sequential quadratic programming (SQP) algorithm (which is generalization of Newton's method for unconstrained optimization) [31]. Figure 5 shows that solutions obtained using SQP and SOCP algorithms are in very good agreement. However, the SOCP algorithm produced solutions very much more quickly and somewhat more accurate, despite the fact that the number of variables involved was much greater ($sdof + 4 \times 3 \times ng \times nele$ cf. $sdof$ when using SQP). To compute solutions for a mesh of 288 elements, the SOCP algorithm typically took only $5 \sim 30$ seconds, compared with $1280 \sim 7000$ seconds when using SQP. Moreover, the SOCP algorithm is able to solve problems up to 152148 of variables with less than 400 seconds CPU time (for the mesh of 4050 elements). It is also important to note that the SOCP algorithm can be guaranteed to identify globally optimal solutions, whereas SQP cannot.

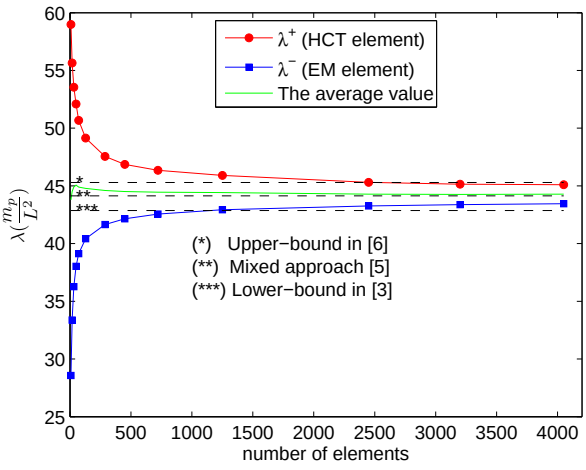

Figure 6: Bounds on the collapse multiplier vs number of elements using SOCP

The performance of the presented numerical limit analysis procedures is further investigated in convergence analysis as shown in Figure 6. It can be observed that both upper and lower bounds converge to the actual collapse multiplier when the size of elements tends to zero. A upper-bound of 45.12 was

achieved by present method, which is slightly smaller than the solution previously obtained in [6]. In comparison with previously obtained lower-bound solution, the present method provides higher solutions than in [3] where quadratic moment fields were used, by 0.6 %.

The next example comprises a square plate with simply supported on all edges. Convergence analysis of collapse load multipliers is shown in Figure 7. It can be seen from the figure that the upper-bound converges to the actual collapse multiplier when relatively small number of elements was used; and the gap between upper and lower bound is considerably smaller than the clamped case. This may be explained by the fact that the displacement filed in this problem does not exhibit a singularity in the form of a so-called hinge along boundary. The solutions obtained by the proposed method are in good agreement with previously achieved bounds. Considering previously obtained upper-bound solutions, the present method provides lower solutions than in [3, 6], by 6.16 % and 0.01 %, respectively. Furthermore, a computed lower-bound of 24.93 was found, which is 0.3 % higher than the best lower-bound found in [3] where quadratic moment fields were used.

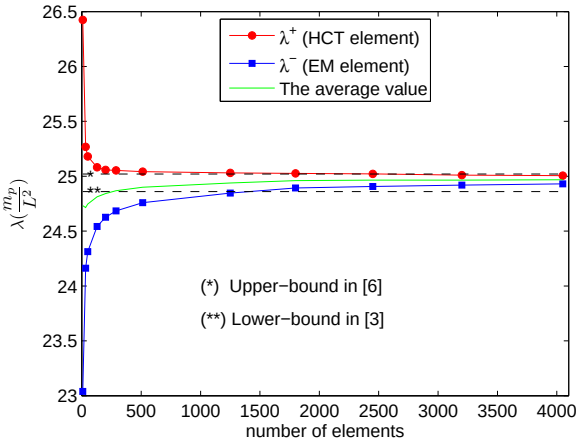

Figure 7: Bounds on the collapse multiplier vs number of elements using SOCP

In the two examples examined above, the computed upper-bounds are slightly

higher than solution in [29] where the Element-Free Galerkin method was used to approximate the displacement filed. However, the presented method can provide very tight lower-bound solutions and based on the computed bounds the actual collapse multiplier can be estimated, e.g. taking the mean value of the obtained upper and lower bounds. For these examples, the computed mean values are in excellent agreement with solutions in [5].

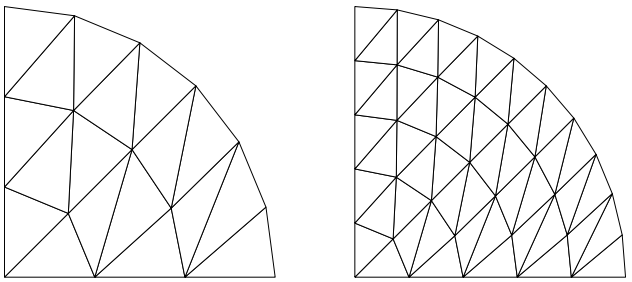

(a) 18 elements (b) 50 elements

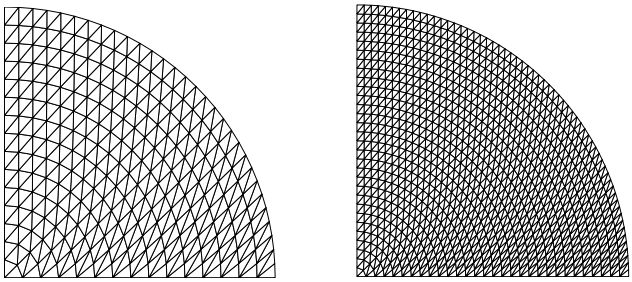

(c) 450 elements (d) 1800 elements

Figure 8: Mesh refinements for a quarter of the circular plate

Further illustration of the method can be made by examining a clamped circular plate, for which the exact solution exists [32], $\lambda = 12.5\ \frac{m_p}{R^2}$ where R is the radius. Mesh refinements for a quarter of the plate are shown in Figure 8.

Figure 9 shows the improvement in the computed collapse load as the problem is refined uniformly. Due to the singularity of the displacement field along the boundary of the plate, the displacement model (HCT) results in a slower convergence than when using the equilibrium model (EM). When 4050 elements were used, the lower-bound was found to be 12.42, just 0.64 % different to the

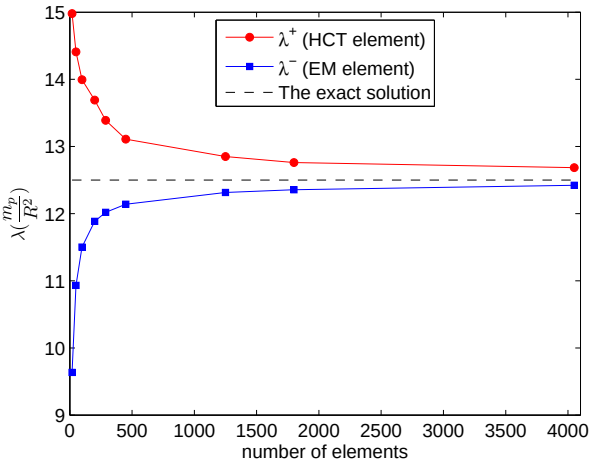

Figure 9: Bounds on the collapse multiplier vs number of elements using SOCP (circular plate)

exact solution.

Finally, an L-shape plate subject to a uniform load was considered. The plate geometry and uniform mesh refinements are shown in Figure 10 and Figure 11, respectively. Collapse load multipliers for various numbers of elements are plotted in Figure 12. The L-shape plate problem exhibits both stress and displacement singularities at the re-entrant corner. This evidently results in a slow convergence and the gap between upper and lower bounds are large despite that fact that a large number of elements was used. For this example, the computed upper-bound was found to be 6.289 which is lower than the best solution obtained previously in [29].

6. Conclusions

The performance of the two novel numerical limit analysis procedures using finite element method in conjunction with second-order cone programming has been investigated. It has been shown that when limit analysis problems are cast in the form of a SOCP, the resulting optimization problems can be solved rapidly by such a efficient interior point algorithm, even though for cases when a very large number of variables involves. The proposed procedures are enable to

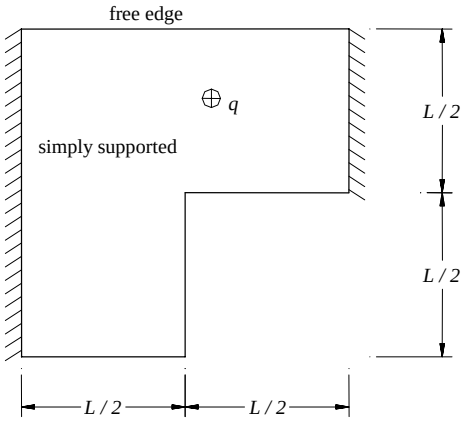

Figure 10: L-shaped geometry

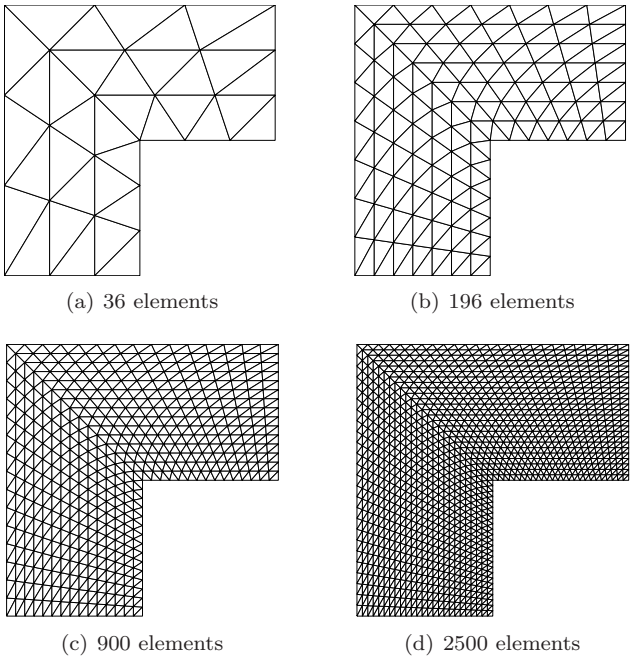

(a) 36 elements (b) 196 elements

(c) 900 elements (d) 2500 elements

Figure 11: Mesh refinement for L-shape plate

provide relatively good bounds on the actual collapse load multiplier since most solutions in existing references were improved. Moreover, the proposed procedures can handle efficiently problems of arbitrary geometry. The only drawback is that the solutions are highly sensitive to the geometry of the finite element

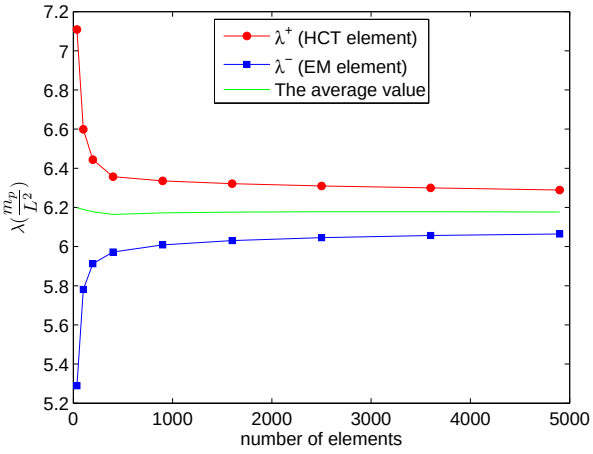

Figure 12: Bounds on the collapse multiplier vs number of elements using SOCP (L-shape plate)

mesh, particularly in the region of stress or displacement singularities. An automatically adaptive mesh refinement scheme can be performed to increase the accuracy of solutions. A well-known benefit from dual structure of limit analysis is that both the stress and velocity fields of the upper and lower bound problem can be determined. It is, therefore, relevant to investigate the performance of an adaptive scheme based on a posteriori error estimate using elemental and edge contributions to the bound gap [22, 23].

References

[1] K. W. Johansen, Yield-line theory, London: Cement and Concrete Association, 1962.

[2] R. H. Wood, Plastic and elastic design of slabs and plates, London: Thames and Hudson, 1961.

[3] P. G. J. Hodge, T. Belytschko, Numerical Methods for the Limit Analysis of Plates, Trans. ASME, Journal of Applied Mechanics 35 (1968) 796–802.

[4] E. Christiansen, S. Larsen, Computations in limit analysis for plastic plates,

International Journal for Numerical Methods in Engineering 19 (1983) 169–184.

[5] K. D. Andersen, E. Christiansen, M. L. Overton, Computing limit loads by minimizing a sum of norms, SIAM Journal on Scientific Computing 19 (1998) 1046–1062.

[6] A. Capsoni, L. Corradi, Limit analysis of plates - a finite element formulation, Structural Engineering and Mechanics 8 (1999) 325–341.

[7] K. Krabbenhoft, L. Damkilde, Lower bound limit analysis of slabs with nonlinear yield criteria, Computers and Structures 80 (2002) 2043–2057.

[8] A. M. Yan, H. Nguyen-Dang, Limit analysis of cracked structures by mathematical programming and finite element technique, Computational Mechanics 24 (1999) 319–333.

[9] A. M. Yan, R. J. Jospin, H. Nguyen-Dang, An enhance pipe elbow element - application in plastic limit analysis of pipe structures, International Journal for Numerical Methods in Engineering 46 (1999) 409–431.

[10] Q. Phan-Hong, H. Nguyen-Dang, Limit analysis of 2D structures using gliding line mechanism generated by rigid finite elements, Collection of papers from Prof. Nguyen-Dang Hungs former students, Vietnam National University, Ho Chi Minh City Publishing house, 2006, pp. 447–460.

[11] R. Clough, J. Tocher, Finite element stiffness matrices for analysis of plates in bending, In: Proceedings of the Conference on Matrix Methods in Structural Mechanics, Ohio,Wright Patterson A.F.B., 1965.

[12] L. S. D. Morley, The triangular equilibrium problem in the solution of plate bending problems, Aero. Quart. 19 (1968) 149–169.

[13] V. F. Gaudrat, A Newton type algorithm for plastic limit analysis, Computer Methods in Applied Mechanics and Engineering 88 (1991) 207–224.

[14] N. Zouain, J. Herskovits, L. A. Borges, R. A. Feijoo, An iterative algorithm for limit analysis with nonlinear yield functions, International Journal of Solids and Structures 30 (1993) 1397–1417.

[15] A. M. Yan, H. Nguyen-Dang, Kinematical shakedown analysis with temperature-dependent yield stress, International Journal for Numerical Methods in Engineering 50 (2001) 1145–1168.

[16] H. Nguyen-Dang, A. M. Yan, D. K. Vu, Duality in kinematical approaches of limit and shakedown analysis of structures, Complementary, duality and symmetry in nonlinear mechanics, Shanghai IUTAM Symposium, Edited by David Gao, 2004, pp. 128–148.

[17] K. D. Andersen, E. Christiansen, M. L. Overton, An efficient primal-dual interior-point method for minimizing a sum of euclidean norms, SIAM Journal on Scientific Computing 22 (2001) 243–262.

[18] E. D. Andersen, C. Roos, T. Terlaky, On implementing a primal-dual interior-point method for conic quadratic programming, Mathematical Programming 95 (2003) 249–277.

[19] Mosek, The MOSEK optimization toolbox for MATLAB manual. http://www.mosek.com, Mosek ApS (2008).

[20] K. Krabbenhoft, A. V. Lyamin, S. W. Sloan, Formulation and solution of some plasticity problems as conic programs, International Journal of Solids and Structures 44 (2007) 1533–1549.

[21] A. Makrodimopoulos, C. M. Martin, Upper bound limit analysis using simplex strain elements and second-order cone programming, International Journal for Numerical and Analytical Methods in Geomechanics 31 (2006) 835–865.

[22] H. Ciria, J. Peraire, J. Bonet, Mesh adaptive computation of upper and lower bounds in limit analysis, International Journal for Numerical Methods in Engineering 75 (2008) 899–944.

[23] J. Munoz, J. Bonet, A. Huerta, J. Peraire, Upper and lower bounds in limit analysis: adaptive meshing strategies and discontinuous loading, International Journal for Numerical Methods in Engineering 77 (2009) 471–501.

[24] J. F. Debongnie, Applying pressures on plate equilibrium elements, Technical report, University of Liege, Belgium.

[25] H. Nguyen-Xuan, J. F. Debongnie, The equilibrium finite element model and error estimation for plate bending, International Congress "Engineering Mechanics Today 2004", Ho Chi Minh City, Vietnam, August 16-20, 2004.

[26] J. F. Debongnie, H. Nguyen-Xuan, C. Nguyen-Hung, Dual analysis for finite element solutions of plate bending, Proceedings of the Eighth International Conference on Computational Structures Technology, B.H.V. Topping, G. Montero and R. Montenegro (Editors), Civil-Comp Press, Stirlingshire, Scotland., 2006.

[27] H. Nguyen-Dang, Direct limit analysis via rigid-plastic finite elements, Computer Methods in Applied Mechanics and Engineering 8 (1976) 81–116.

[28] E. Christiansen, Limit analysis of collapse states, Handbook of Numerical Analysis, vol IV, volume IV, chapter II, pages 193312. North Holland Amsterdam, 1996.

[29] C. V. Le, M. Gilbert, H. Askes, Limit analysis of plates using the EFG method and second-order cone programming, International Journal for Numerical Methods in Engineering 78 (2009) 1532–1552.

[30] H. Nguyen-Dang, J. A. Konig, A finite element formulation for shakedown problems using a yield criterion of the mean, Computer Methods in Applied Mechanics and Engineering 8 (1976) 179–192.

[31] C. V. Le, H. Nguyen-Xuan, H. Nguyen-Dang, Dual limit analysis of bending plates, Proceeding of Third International Conference On Advanced Computational Methods In Engineering, Ghent - Belgium, 2005.

[32] H. Hopkins, A. Wang, Load-carrying capacities for circular plates of perfectly-plastic material with arbitrary yield condition, Journal of the Mechanics and Physics of Solids 3 (1954) 117–129.